Remote Estimation of Net Ecosystem CO_2 Exchange in Crops: Principles, Technique Calibration and Validation

Anatoly A. Gitelson[1,2], Andrés Viña[1], Shashi B. Verma[2], Donald C. Rundquist[1,2], Timothy J. Arkebauer[3], Galina Keydan[1], Bryan Leavitt[1], Veronica Ciganda [1,3], George G. Burba[2], and Andrew E. Suyker[2]

[1]Center for Advanced Land Management Information Technologies (CALMIT), University of Nebraska-Lincoln, 102 Nebraska Hall, Lincoln, NE 68588-0517. [2]School of Natural Resources, University of Nebraska-Lincoln, [3]Department of Agronomy, University of Nebraska-Lincoln.

Abstract

Accurate and synoptic estimation of spatially distributed CO_2 fluxes is of great importance for regional and global studies of carbon balance. A technique solely based on remotely sensed data was developed and tested for estimating net ecosystem CO_2 exchange (NEE) in maize and soybean. The model is based on the reflectance in two spectral channels: the near-infrared and either the green or red-edge around 700 nm. The technique provides accurate estimations of mid-day NEE in both crops under either rainfed or irrigated conditions, explaining more than 85% of NEE variation in maize and more than 81% in soybean, and shows great potential for remotely tracking crop NEE.

Introduction

The importance of studying vegetation dynamics has been recognized for decades (e.g., Box, 1978). A key driver has been the interest in understanding the patterns of terrestrial vegetation productivity and their relationships with global biogeochemical cycles of carbon and nitrogen (e.g., Cao & Woodward, 1998). Studies in mid and high latitude forests (e.g., Wofsy et al., 1993) and grasslands (e.g., Suyker and Verma, 2001) have documented the role of these ecosystems in the global carbon cycle. The potential of agroecosystems to sequester carbon has also received considerable scientific attention in the last few years (e.g., Lal et al., 1998), particularly because agroecosystems are the most pervasive anthropogenic biome. Within the United States, there are approximately 1.7 million km^2 of cropland, with 43% occurring within eight agricultural states: Indiana, Illinois, Iowa, Minnesota, North Dakota, South Dakota, Nebraska, and Kansas. The main crops in this core region are: maize for grain or seed (70%), soybean (61%), wheat for grain (50%), sorghum (48%), and alfalfa (40%) (USDA-NASS, 1999).

In agroecosystems across the world, field studies have used tower-based eddy covariance techniques to provide information on seasonal dynamics and inter-annual variation of net ecosystem CO_2 exchange (NEE) (e.g., Baldocchi et al., 1988). These instruments provide NEE data from a small footprint area but scaling-up beyond the footprint to an entire region is challenging. Remote sensing has a potential to help estimate these fluxes on a regional basis.

Models of terrestrial net primary productivity (NPP) can be classified into two broad categories according to the way they depict the absorption of solar radiation and its conversion into dry matter. Using solar radiation as an input, these models either compute the absorbed solar radiation directly - the Production Efficiency Models (PEMs) - or the amount of leaves, as

---

2nd International Workshop on Remote Sensing of Vegetation Fluorescence, November 17-19, 2004, Montreal, Canada. CD-Rom, ESA WPP-242
Gitelson (gitelson@calmit.unl.edu), Tel 1-402-472-8386

represented by the leaf area index (LAI), used to absorb solar radiation—the Canopy Photosynthesis Models. PEMs are based on the approach of Kumar and Monteith (1981):

$$NPP \propto LUE*fAPAR*PAR \quad (1)$$

where PAR is the incident photosynthetically active radiation (PAR) in a time period, fAPAR is the fraction of PAR absorbed by a vegetation canopy, and LUE is the light use efficiency or the efficiency of conversion of absorbed light into aboveground biomass.

Analysis of performance of twelve global NPP models (Ruimy *et al.*, 1999) has revealed generally high correlations between annual NPP and annual absorbed PAR (APAR = fAPAR*PAR). Thus, the variations of NPP within models depend primarily on variations of APAR and the variations in LUE are second-order effects. Comparison of the models (Ruimy *et al.*, 1999) revealed that NDVI-derived APAR is significantly lower than the independently modeled APAR by a ***consistent global discrepancy of 28%***. They concluded that it was not possible to determine the primary cause of this discrepancy but that the answer to this question should come from ***improvements in remote sensing***.

In the vegetative stage, Kumar and Monteith (1983) found linear relationships between fAPAR and the simple ratio spectral index. However, Hatfield et al., (1984) and Gallo et al., (1985) reported that during the reproductive and senescence stages, the slope of this relationship was significantly different. In these stages, the canopy still intercepts the incoming radiation, but the leaves contain less photosynthetic pigments, which leads to a decrease in the values of the index. Ruimy et al. (1994) also underscored the fact that the linear relationship between fAPAR and NDVI is an approximation, and it is only valid for vegetation during the growing stage.

An important feature of the NDVI/fAPAR relationship is the significant decrease in the sensitivity of NDVI when fAPAR exceeds 0.7 (Asrar et al., 1984; Asrar et al., 1992, Goward and Huemmrich, 1992; Roujean and Breon 1995; Walter-Shea et al., 1997). This relationship is likely dependent on crop status and genotype. Thus, one of the the main problems of remote NPP assessment is caused by the uncertainty of the NDVI/FAPAR relationship, which is normally assumed to be linear and constant.

According to Monteith (1972), the LUE is a relatively conservative value among plant formations of the same metabolic type. However, it can vary with phenological stage, climatic condition, temperature, and water stress (Jarvis and Leverenz, 1983). Ruimy et al. (1994) ran the model with minimal and maximal conversion efficiencies for each vegetation class. These values varied about five fold for crops. Minimal and maximal prediction of NPP were 27 and 150 $Ct_c \cdot yr^{-1}$, respectively, i.e. a ratio of nearly 1 to 6. We also have found that, at least in maize, LUE variation is not a second-order effect, and thus cannot and should not be neglected (Gitelson et al., 2003a). Therefore, the uncertainty of the estimation of terrestrial NPP with Monteith's model is considerable, when no information about factors influencing LUE is introduced.

A technique was developed and tested in two irrigated maize fields to remotely estimate mid-day canopy CO_2 fluxes (Gitelson et al., 2003a). This technique was based on the assumption that CO_2 fluxes and total chlorophyll content in the crop canopy are closely related (e.g., Lieth and Whittaker, 1975). CO_2 fluxes measured with a tower eddy covariance system were linearly related to the difference between reciprocal reflectance either in the green (near 550 nm) or the red edge (around 700 nm) spectral regions and reciprocal reflectance in the near infrared region (NIR).

The goals of this study were: (1) to determine how existing remote sensing techniques allow us to estimate NEE in crops; (2) to establish a relationship between NEE, total chlorophyll content in crops and remotely sensed reflectance for maize and soybean, and (3) to test the accuracy and robustness of

the remote sensing technique, developed for chlorophyll content retrieval, in the estimation of NEE in crops.

Methods

The study took place at a University of Nebraska-Lincoln research facility located 58 km northeast of Lincoln NE, U.S.A., and consists of three agricultural fields; the first two (here denoted as Fields 1 and 2, respectively) are 65-ha fields equipped with center pivot irrigation systems. The third field (denoted as Field 3) is of approximately the same size, but relies entirely on rainfall. All three fields were uniformly tilled prior to the initiation of the research program, and have not been further tilled. Field 1 is under continuous maize, while Fields 2 and 3 are under maize-soybean rotation.

Micrometeorological eddy covariance data collection began on May 25, 2001 at Fields 1 and 2, and on June 13, 2001, at Field 3. To have sufficient upwind fetch (in all directions), eddy covariance sensors were mounted at 3 m above the ground while the canopy was shorter than 1 m, and later moved to a height of 6.2 m until harvest (details are given in Suyker et al., 2004). Mid-day NEE values were computed by integrating the CO_2 fluxes collected by the eddy covariance tower from 10:00am to 15:00pm.

Both incoming PAR and PAR reflected by the canopy were measured with Licor point quantum sensors at a height of 6 m. PAR transmitted through the canopy was measured with Licor line quantum sensors at about 2 cm above the soil surface. PAR reflected by the soil was measured with Licor line quantum sensors at about 12 cm above the soil surface.

Within each study site, six small (20m x 20m) plot areas were established for detailed process-level studies. Six locations per field were selected using fuzzy-k-means clustering, applied to seven layers of previously collected, spatially dense information (elevation, soil type, electrical conductivity, soil organic matter content, digital aerial photography and four years of yield map data). The resulting intensive measurement zones (IMZs) represent all major occurrences of soil and crop production zones within each field.

Plant populations were determined for each IMZ. On each sampling date, plants from a 1m length of either of two rows within each IMZ were collected and the total number of plants recorded. Collection rows were alternated on successive dates to minimize edge effects on subsequent plant growth. Plants were transported on ice to the laboratory. In the lab, plants were dissected into green leaves, dead leaves, stems, and reproductive organs. The green leaves were processed through an area meter (Model LI-3100, Li-Cor, Inc., Lincoln NE) and the leaf area per plant was determined. For each IMZ, the green leaf area per plant was multiplied by the plant population (# plants m^{-2}) to obtain a green LAI. Green LAI data at the six IMZs were averaged to obtain a field-level value. Green LAI calculated in this manner did not differ significantly from the one calculated using an IMZ area-weighted average. All plant parts were dried to constant weight in a 70 °C dryer. Field-level green leaf biomass was then calculated in a manner analogous to LAI. Standard deviations of the destructive sampling of LAI ranged from 0.05 m^2/m^2 at the beginning of the growing season (DOY 163) to 0.48 m^2/m^2 before the peak of maximum LAI (around day of the year 180).

Leaf reflectance spectra in the range 400 to 900 nm were measured in situ by an Ocean Optics radiometer, equipped with a leaf clip. Leaf chlorophyll content was retrieved from reflectance spectra using a non-destructive technique for chlorophyll estimation (Gitelson and Merzlyak, 1994; 1996). Reflectance in two spectral bands, the red edge between 700 and 720 nm and in the near infra-red (NIR) between 760 and 800 nm, were used in the model:

$$Chl=a+b[(\rho_{NIR}/\rho_{red\ edge})-1] \quad (2)$$

To calibrate the model, Chl content was measured analytically in the lab and the coefficients *a* and *b* were determined for both species (i.e. maize and soybean).

Spectral measurements at the canopy/community level were made using hyperspectral radiometers mounted on "Goliath", an all-terrain sensor platform (Rundquist et al., 2004). A dual-fiber system, with two inter-calibrated Ocean Optics USB2000 radiometers, was used to collect radiometric data in the range 400-1100 nm with a spectral resolution of about 1.5 nm. Radiometer #1, equipped with a 25° field-of-view optical fiber was pointed downward to measure the upwelling radiance of the crop (L_λ^{crop}). Radiometer #2, equipped with an optical fiber and cosine diffuser (yielding a hemispherical field of view), was pointed upward to simultaneously measure incident irradiance (E_λ^{inc}). The inter-calibration of the radiometers was accomplished, in order to match their transfer functions, by measuring the upwelling radiance (L_λ^{cal}) of a white Spectralon (Labshere, Inc., North Sutton, NH) reflectance standard simultaneously with incident irradiance (E_λ^{cal}). To mitigate the impact of solar elevation on radiometer intercalibration, the anisotropic reflectance from the calibration target was corrected in accord with Jackson et al (1992). Percent reflectance (ρ_λ) was computed as:

$$\rho_\lambda = (L_\lambda^{crop}/E_\lambda^{inc})\,(E_\lambda^{cal}/L_\lambda^{cal})*100*\rho_\lambda^{cal} \quad (3)$$

where L_λ^{crop} and E_λ^{inc} are the outputs of the downward (upwelling radiance of crop) and upward (incident irradiance) pointing instruments, respectively; ρ_λ^{cal} is the reflectance of the Spectralon panel linearly interpolated to match the band centers of each radiometer; L_λ^{cal} is the output of the downward looking instrument when measuring the upwelling irradiance of the Spectralon panel; E_λ^{cal} is the output of the upward pointing instrument measuring incident irradiance during the time of calibration by means of the Spectralon panel. L_λ^{crop}, E_λ^{inc}, L_λ^{cal} and E_λ^{cal} are in digital numbers per second, corrected for dark current.

Our ultimate goal was to eliminate the need to use a calibration panel after each reflectance measurement and to avoid errors due to atmospheric variability during data collection. The use of two inter-calibrated hyperspectral radiometers allows simultaneous measurement of downwelling irradiance and upwelling target radiance. Therefore, it is possible to compute the radiance reflectance of a target during times when the incident radiation is highly variable. Such situations are difficult, if not impossible, when using one radiometer and measuring a reference panel after each target scan. The dual-fiber approach results in rapid measurement and minimal error due to variation in irradiation condition (Rundquist et al., 2004).

One critical issue with regard to the dual-fiber approach is that the transfer functions of both radiometers must be identical. We tested our Ocean Optics instruments under laboratory and field conditions; over a four-hour period the standard deviations of the ratio of the two transfer functions did not exceed 0.004.

Our data were collected with the sensors configured to take fifteen simultaneous upwelling radiance and downwelling irradiance measurements, which were internally averaged and stored as a single data file. Radiometric data were collected close to solar noon (between 11am and 1pm), when changes in solar zenith angle were minimal. On each measurement date, six randomly selected plots were established per field, each with six randomly selected sampling points. Measurements took about 5 minutes per plot and about 30 minutes per field. The two radiometers were inter-calibrated immediately before and immediately after measurement in each field.

Reflectances in the range 545 to 565 nm, ρ_{green}, and in the range 841 to 876 nm, ρ_{NIR}, used in the analyses were calculated in the spectral channels of the Moderate Resolution Imaging Spectrometer (MODIS) onboard the Terra and Aqua satellites, and in the range 700 to 710, $\rho_{red\ edge}$, of the Medium Resolution Imaging Spectrometer (MERIS) onboard the polar orbiting Envisat Earth Observation Satellite.

Spectral reflectance measurements were made within an area of ~0.8 ha for each of the three fields. A total of 36 points within these areas were sampled per measurement date and field, and the median was calculated. Since eddy covariance measurements represent NEE of the entire fields, while reflectance data were sampled in specific areas of the field, a test of field homogeneity was needed to assess if the reflectance sampling areas were representative of the entire fields. For this, we used imagery acquired during the 2002 growing season (on June 21, June 27, July 12, July 15, September 7 and September 17) by an AISA (Oulu, Finland) hyperspectral imaging system, programmed to acquire 35 spectral bands between 400 and 900 nm. Measurements were carried out from an altitude of ~1000m, providing a spatial resolution ~3m/pixel. The index $[\rho_{NIR}/\rho_{700\text{-}710nm})\text{-}1]$, which is a proxy of green LAI (Gitelson et al., 2003b), was calculated for each of these images, and the values from the entire fields and from the spectral reflectance sampling areas were compared on a per field and date basis, using a two-sample T-test, after checking for variance homogeneity. Field average values of this index that are significantly different from those of the spectral reflectance sampling areas would mean that the spectral sampling areas are not representative of the fields, and thus an over- or under-estimation of the remote NEE estimate might occur. With the exception of Field 3 on September 7, 2002, no statistically significant differences were obtained (Table 1). Therefore, the spectral reflectances for sampled areas were representative of the entire fields. For September 7, 2002 the spectral sampling area of Field 3 showed a statistically significant underestimation of the green LAI, as compared to the entire field, and this might translate into an underestimation of the remote estimation of NEE. This only occurred for this field and date.

Results and Discussion

Temporal progressions of mid-day NEE in maize and soybean fields during the growing season are shown for irrigated maize (Fig. 1A) and irrigated soybean (Fig. 1B). NEE contains two types of variation, low frequency variation, which relates to the phenological development of the crops and high frequency variation, which relates to the changes in radiation conditions.

First, we tried to understand if the assumption of a constant LUE holds for the crops studied. In Fig. 2 we plotted NEE as measured by the tower-based eddy covariance technique versus the product of NDVI and PAR. The NDVI was used here as a proxy of fAPAR (e.g., Sellers, 1992; Ruimy et al., 1994; Prince & Goward, 1995, Running et al., 2000). The product NDVI*PAR explains only 61% of the NEE variation in maize and even less (56%) in soybean. For both species together, the product NDVI*PAR explains about 53% of NEE variation.

We calculated LUE = NEE/(fAPAR*PAR) and plotted it versus day of the year (DOY) - Figure 3. LUE showed considerable variation, with minimal values at the beginning of the growing season and maximal values during the middle of the growing season (around 0.002 mg/mmol for maize and 0.001 mg/mmol for soybean). During the reproductive and senescent stages, LUE dropped conspicuously. It is worth noting that the temporal behavior of LUE mimicked the temporal variability of green vegetation cover in crops (e.g., Viña et al., 2004).

Table 1. T-test values and their respective P-values for the comparison of means of the index $[(\rho_{NIR}/\rho_{Red\text{-}edge})\text{-}1]$ calculated from reflectance data acquired by the AISA system during the 2002 growing season, within the reflectance sampling areas and the entire fields.

Field	Date	T-test	P-value
Irrigated Maize (Field 1)	6/21/02	0.757	0.462*
	6/27/02	0.913	0.377
	7/12/02	1.299	0.215
	7/15/02	2.012	0.064
	9/7/02	1.159	0.266
	9/17/02	1.628	0.126
Irrigated Soybean (Field 2)	6/21/02	0.283	0.781
	6/27/02	0.185	0.856
	7/12/02	0.556	0.587
	7/15/02	0.615	0.549
	9/7/02	-0.283	0.781
	9/17/02	-0.709	0.490
Rainfed Soybean (Field 3)	6/21/02	-0.451	0.671*
	6/27/02	0.059	0.955*
	7/12/02	-0.211	0.836
	7/15/02	-1.846	0.092
	9/7/02	-3.222	0.008#
	9/17/02	-2.081	0.083*

*Two-sample T-test assuming unequal variances
#Statistically significant difference

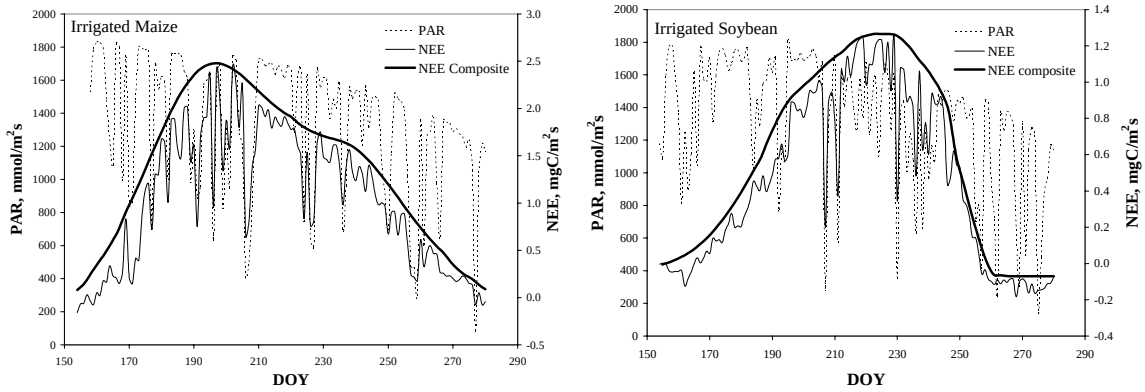

Figure 1. Temporal progression of measured mid-day NEE (thin line), 9-day maximal-value composite (solid line) and incident PAR (dotted line) in irrigated and rainfed maize (left panel) and soybean (right panel) fields during the 2002 growing seasons.

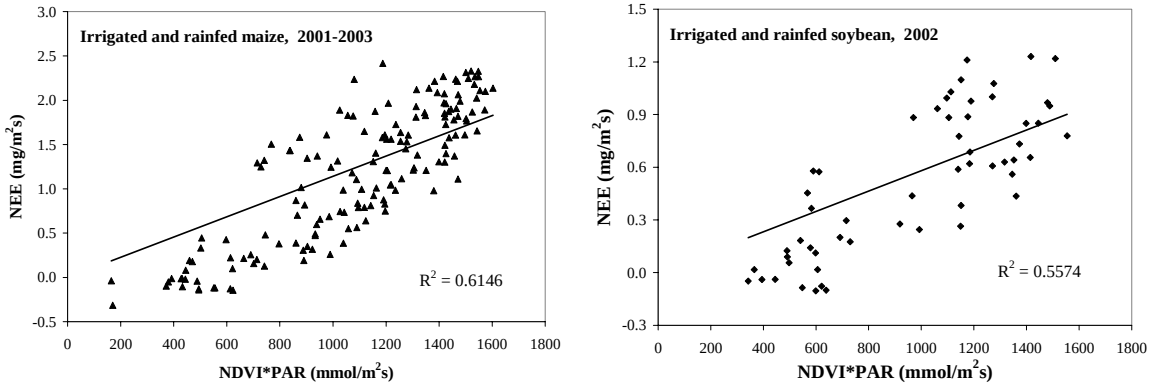

Figure 2. NEE plotted versus the product of NDVI and incident PAR for irrigated and rainfed maize (left panel, five irrigated and two rainfed fields, 2001-2003), and soybean (right panel, one irrigated and one rainfed field). It can be seen that the assumption of constant light use efficiency value does not hold for either maize or soybean.

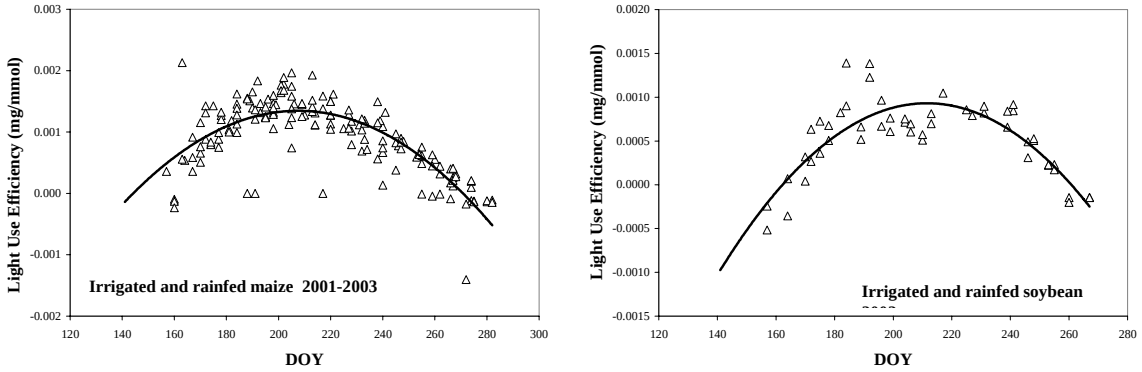

Figure 3. Temporal behavior of light use efficiency determined as a ratio NEE/(PAR*fAPAR) for irrigated and rainfed maize (2001-2003), and irrigated and rainfed soybean (2002). It can be seen that the assumption of a constant light use efficiency value does not hold for either species.

The photochemical reflectance index (PRI) has been proposed and used as an indicator of photosynthetic activity and as a proxy of LUE (Gamon et al., 1992, Rahman et al., 2004).

$$PRI = (\rho_{531}-\rho_{570})/(\rho_{531}+\rho_{570}) \quad (4)$$

where R_{531} is reflectance at wavelength 531 nm and R_{570} is reflectance at 570 nm.

We calculated a scaled PRI as sPRI = (1+PRI)/2 (as suggested by Rahman et al., 2004) and plotted NEE as a function of the product PAR*NDVI*sPRI (Figure 4). For both species, the linear relationship between NEE and PAR*NDVI*sPRI is slightly better than that between NEE and PAR*NDVI (i.e. r^2 became 0. 6585 vs. 0.6146 in maize and 0.6012 vs. 0.5574 in soybean), but no significant improvement was observed. Thus, it is evident that sPRI is not a proxy of LUE in the crops studied, and new approaches are needed to estimate accurately NEE in crops.

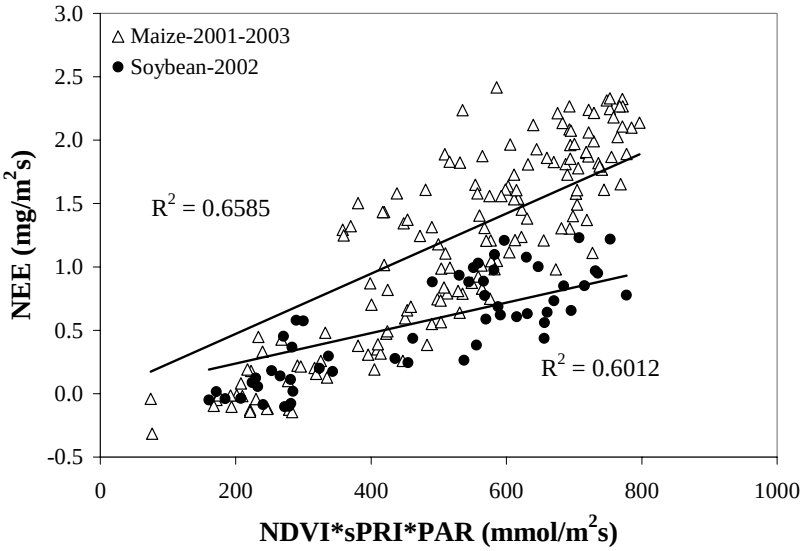

Figure 4. NEE versus the product of NDVI, incident PAR and sPRI for irrigated and rainfed maize (left panel) and soybean (right panel). The relationship is slightly better than that of NEE vs. NDVI*PAR (Figure 2), but the dispersion of points away from the line of best fit is substantial. Thus, sPRI was not a proxy of LUE in crops studied.

The low frequency variation in NEE is associated with crop phenology and physiological status (see maximal-value composite in Fig. 1). NEE is a function of the efficiency of the leaf's light-harvesting apparatus (i.e., fAPAR), amount of PAR captured by the leaf chlorophyll (APAR = PAR*fAPAR) and the capacity of the leaf to export or utilize the product of photosynthesis (i.e., LUE). Both fAPAR and LUE are closely related to the chlorophyll content in a canopy. fAPAR*LUE depends on the amount and distribution of photosynthetic biomass, the primary source of variability in chlorophyll and leaf physiology (Sellers et al., 1992). It has been shown that low frequency variation in NPP and NEE in cropland and grassland is closely related to leaf area index (LAI) and total chlorophyll content in the canopy (e.g., Leith and Whittaker 1975). They suggested that "chlorophyll content and leaf area index are more directly expressive of the photosynthetic apparatus of the community". Their suggestion was found to hold true for irrigated and rainfed maize (Suyker *et al.*, 2004).

Our approach to estimate NEE remotely is based on the hypothesis that the ***total chlorophyll content in crops relates closely to low frequency variation in NEE***. The relationship between measured NEE and the product of PAR and total chlorophyll content in both maize and soybean is presented in Figure 5. The close relationship between NEE and total chlorophyll content shows that the best way to estimate remotely NEE for crops may be found through the estimation of total chlorophyll content.

Retrieving chlorophyll content (Chl) from both leaves and a canopy based on reflectance is quite complicated due to the saturation of red reflectance, even at low Chl values. In the red spectral range, as used in NDVI-like vegetation indices, the specific absorption coefficient of chlorophylls (α^*_{red}) is high (Lichtenthaler 1987) while the depth of light penetration into the leaf is low (e.g., Kumar and Silva 1973). As a result, even low amounts of pigments or small LAI (around 2) are sufficient to saturate absorption in the red spectral region (Kanemasu, 1974; Buschmann and Nagel, 1993; Gitelson *et al.*, 2003c), which explains the essentially nonlinear behavior of NDVI as a function of LAI.

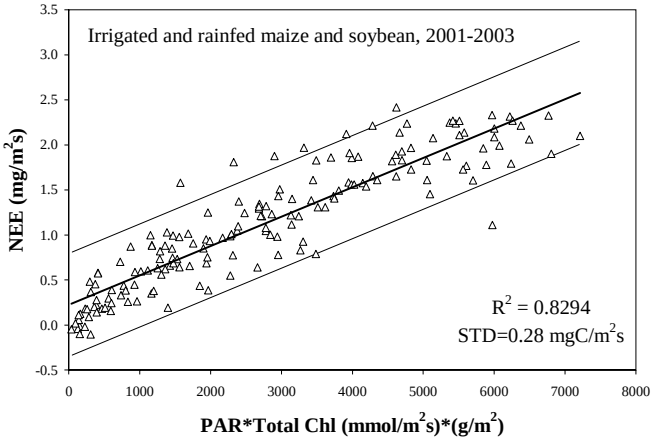

Figure 5. NEE versus PAR*Total chlorophyll content in the canopy. Total chlorophyll content was calculated as the product of LAI and leaf chlorophyll content. The product of PAR and total chlorophyll content was responsible for more than 82% of NEE variation in both species.

Specific absorption coefficients of chlorophylls in the green and the red edge (around 700 nm) spectral regions, located quite far from their main chlorophyll absorption bands, are much smaller than in the red region: α^*_{green} and $\alpha^*_{red\ edge}$ are only about 2-5% of α^*_{red} (e.g., Lichtenthaler, 1987). In these spectral ranges, reflectance decreases steadily with an increase in Chl content (Thomas and Gaussman, 1977; Buschmann and Nagel, 1993; Gitelson *et al.*, 1996) and reciprocal reflectance is linearly related to leaf Chl content in a wide range of its variation from 10 to more than 800 mg/m^2 (Gitelson et al., 2003c).

The reciprocal reflectance of a leaf may be expressed as:

$$\rho^{-1} = (\alpha_{Chl} + \alpha_0)/b_b \qquad (5)$$

where α_{Chl} is absorption coefficient of chlorophyll, α_0 is absorption coefficient of pigments other than chlorophyll, and b_b is backscattering coefficient.

To retrieve Chl content from reflectance spectra one needs to isolate α_{Chl}, i.e. to find a function of reflectance that is closely related to α_{Chl}. A conceptual model was developed that relates leaf pigment content (C) with reflectance at three wavelengths (Gitelson et al., 2001; 2002; 2003c):

$$C \propto [\rho^{-1}(\lambda_1) - \rho^{-1}(\lambda_2)]/\rho(\lambda_3) \qquad (6)$$

were λ_1 is a wavelength where reciprocal reflectance is maximally sensitive to the absorption of a pigment of interest (e.g., α_{Chl}), but it is also influenced by the absorption of other pigments (α_0). λ_2 is a wavelength where reciprocal reflectance is affected mainly by absorption of pigments other than the pigment of interest (α_0), and λ_3 is a wavelength where reflectance depends mainly on leaf structure and thickness, i.e., scattering by leaf (b_b).

Subtraction of $\rho^{-1}(\lambda_2)$ from $\rho^{-1}(\lambda_1)$ allowed isolating the absorption of the pigment of interest; however, item $[\rho^{-1}(\lambda_1) - \rho^{-1}(\lambda_2)]$ was still hyperbolically related to leaf scattering. To decrease this effect and isolate the absorption coefficient of the pigment of interest, the difference was multiplied to $\rho(\lambda_3)$ that is linearly related to b_b. This conceptual model has been used to estimate leaf contents of chlorophyll, carotenoids, anthocyanin, and, recently, flavenoids (Gitelson et al., 2001; 2002; 2003c).

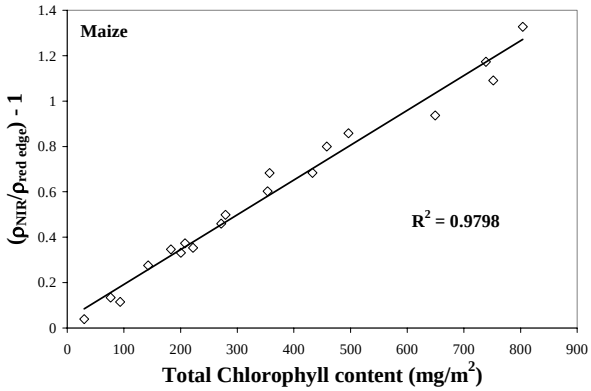

Figure 6. Non-destructive chlorophyll retrieval from leaf reflectance spectra. A model in the form $[\rho^{-1}_{red\ edge} - \rho^{-1}_{NIR}]*\rho_{NIR}$ is plotted versus chlorophyll content in maize leaves as measured analytically in the lab.

For leaf Chl content estimation, λ_1 is either in the green (around 550 nm) or the red edge (near 700 nm) ranges and ρ^{-1}_{green} and $\rho^{-1}_{red\ edge}$ are related to total absorption. λ_2 is in the near infra-red range and ρ^{-1}_{NIR} is related to leaf non-photosynthetic absorption. The differences (ρ^{-1}_{green} - ρ^{-1}_{NIR}) and ($\rho^{-1}_{red\ edge}$ - ρ^{-1}_{NIR}) are closely related to Chl absorption but are also influenced by leaf scattering (Gitelson et al., 2003c). Thus, Chl retrieval depends on leaf thickness, structure and density. To minimize this effect, the differences (ρ^{-1}_{green} - ρ^{-1}_{NIR}) and ($\rho^{-1}_{red\ edge}$ - ρ^{-1}_{NIR}) were multiplied by reflectance in the NIR range that depends mainly on leaf scattering. In Figure 6 comparisons of analytically measured Chl content in maize and soybean leaves and estimated by the model Chl $\propto [\rho^{-1}_{red\ edge} - \rho^{-1}_{NIR}]*\rho_{NIR}$ are shown. The model was able to non-destructively estimate Chl content ranging from 29 to 879 mg/m^2, with a root mean square error of less than 54 mg/m^2.

The generic model $[\rho^{-1}(\lambda_1) - \rho^{-1}(\lambda_2)]*\rho(\lambda_3)$ with λ_1 either in the green (around 550 nm) or the red edge (near 700 nm) ranges and $\lambda_2 = \lambda_3$ in NIR range was found to be closely related to green LAI; the model described more than 95% of LAI variability and was able to predict LAI ranging between 0 and more than 6 with RMSE of less than 0.5 (Gitelson *et al.*, 2003b). Thus, we hypothesize that this model is related to total chlorophyll content in the canopy, determined as the product of leaf Chl content (Chl_{leaf}) and LAI.

$$\text{Total Chl} = Chl_{leaf}*LAI \propto [\rho^{-1}_{green} - \rho^{-1}_{NIR}]*\rho_{NIR} = [(\rho_{NIR}/\rho_{green})-1] \quad (7a)$$

$$\text{Total Chl} = Chl_{leaf}*LAI \propto [\rho^{-1}_{red\ edge} - \rho^{-1}_{NIR}]*\rho_{NIR} = [(\rho_{NIR}/\rho_{red\ edge})-1] \quad (7b)$$

Taking into account that the (total Chl*PAR) is closely related to NEE (Fig. 5), the Carnegie-Ames-Stanford Approach

$$NEE \propto NDVI*PAR*LUE*g(T)*h(W) \quad (8a)$$

can be transformed as follows:

$$NEE \propto \text{Total Chl}*PAR*g(T)*h(W) \quad (8b)$$

where $g(T)$ and $h(W)$ are functions that account for effects of temperature and water stress.

This approach was tested in 2001 through 2003 for irrigated and rainfed maize and soybean. Figure 7 shows the relationship between total Chl content in maize and soybean canopies and the models (7a) and (7b). The models are responsible for more than 91% of chlorophyll variation and are able to accurately estimate Chl content.

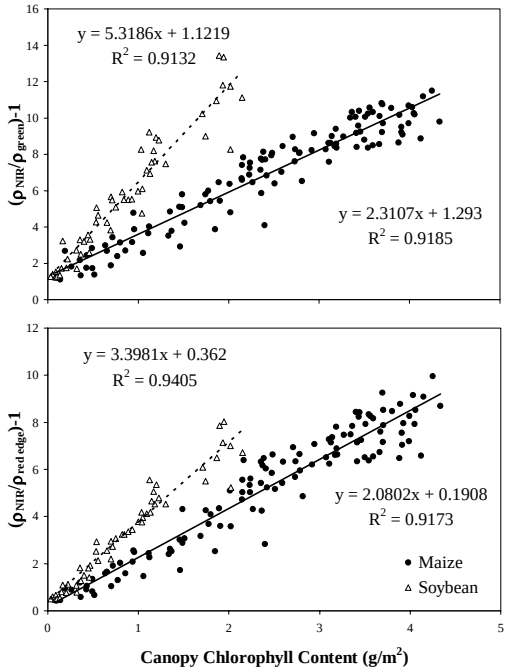

Figure 7. Retrieval of total chlorophyll content in maize and soybean canopies. Models in the form $[(\rho_{NIR}/\rho_{red\ edge}) - 1]$ and $[(\rho_{NIR}/\rho_{green}) - 1]$ are plotted versus canopy chlorophyll content determined as the product of leaf Chl content and LAI.

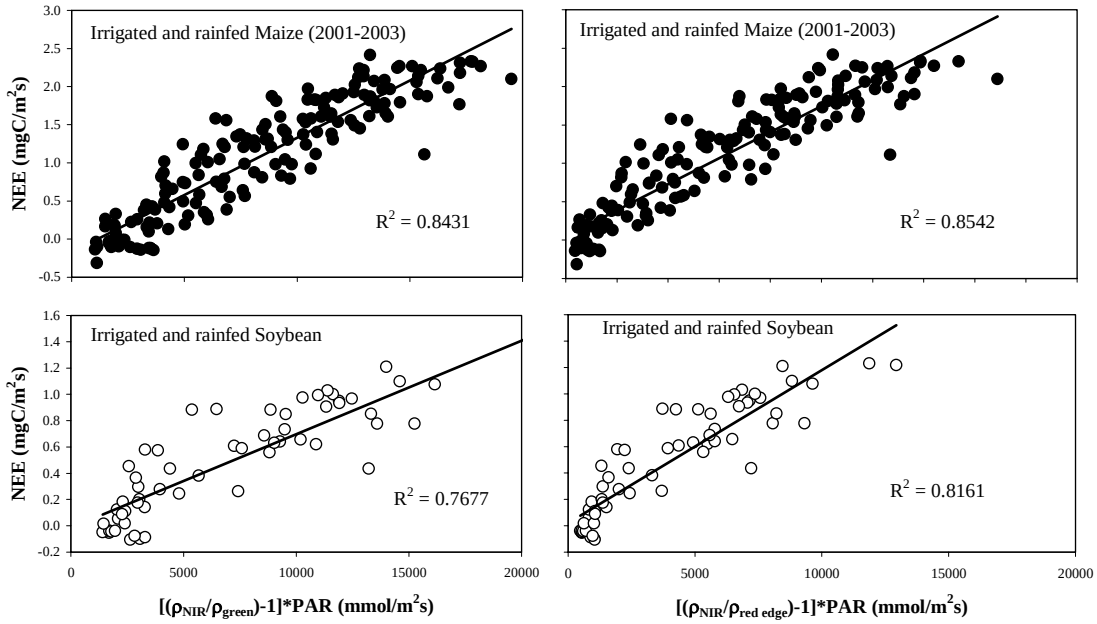

Figure 8. Relationship between NEE and the product $PAR*(\rho_{NIR}/\rho_{green} -1)$ and $PAR*(\rho_{NIR}/\rho_{red\ edge} -1)$ for irrigated and rainfed maize and soybean.

To test our hypothesis that models for total chlorophyll content retrieval might be used for NEE estimation in crops, we analyzed relationships between NEE and the products PAR*(ρ_{NIR}/ρ_{green} -1) and PAR*($\rho_{NIR}/\rho_{red\ edge}$ -1). Figure 8 shows these relationships for irrigated and rainfed maize and soybean.

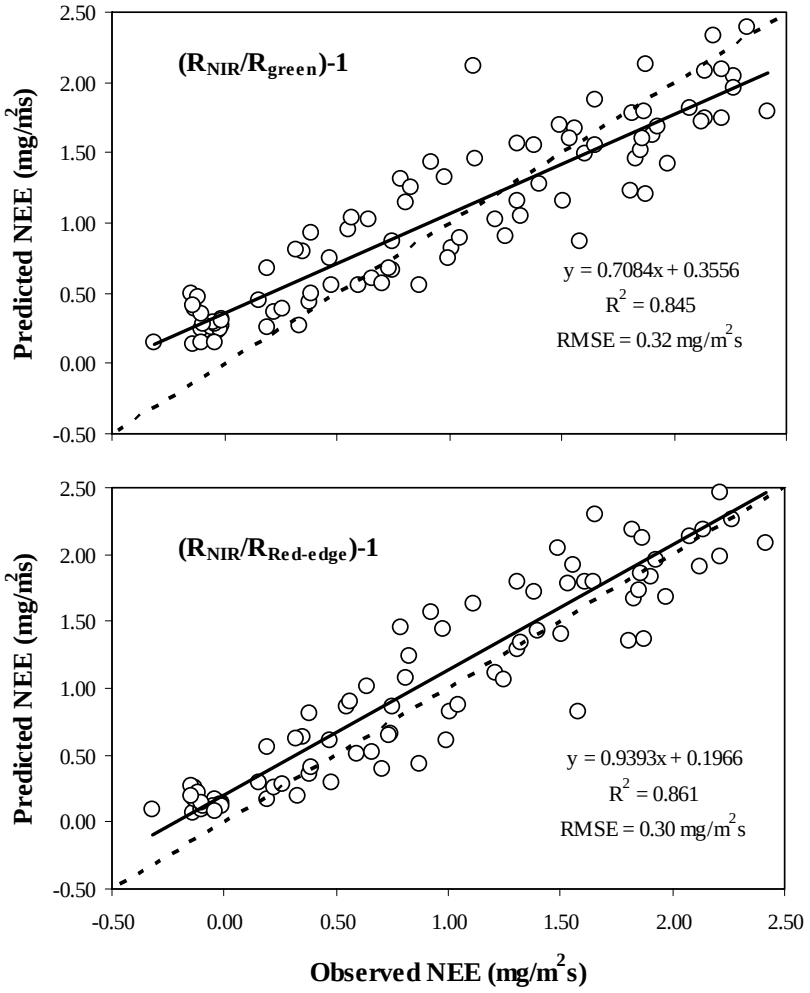

Figure 9. Relationship between NEE predicted by the models (ρ_{NIR}/ρ_{green} -1) and ($\rho_{NIR}/\rho_{red\ edge}$ -1) and observed NEE for irrigated and rainfed maize.

Both models were closely related to NEE in maize and soybean, however, the ($\rho_{NIR}/\rho_{red\ edge}$ -1) was more precise than the (ρ_{NIR}/ρ_{green} -1) explaining more than 81% of NEE variability in soybean and 85% in maize. It is important to note that both models (7a and 7b) are more a measure of total Chl content in the canopy than NEE. The coefficient of determination, r^2, of the linear relationship ($\rho_{NIR}/\rho_{red\ edge}$ -1) vs. total Chl was 0.94 for soybean and 0.91 for maize while the r^2 for {NEE vs. ($\rho_{NIR}/\rho_{red\ edge}$ -1)} was 0.81 for soybean and 0.85 for maize. This is understandable, considering that with the exception of Chl content, NEE is affected by crop stresses - functions of g(T) and h(W) in equations (8). If these stresses affect crop Chl content, the models (equation 7a and b) describe it quite accurately. If short-term stresses do not affect Chl content, then the models fail to detect such stresses.

The models were validated for maize using an independent data set. Calibration of the models has been done using data obtained in irrigated and rainfed fields in 2001 and 2002. Reflectance data obtained in 2003 were used to predict NEE in 2003 using the above calibration. Then, the predicted NEE values were compared with those actually measured in 2003 and the results of the comparison are shown in Figure 9. As was the case with model calibration (Figure 8), the model ($\rho_{NIR}/\rho_{red\ edge}$ -1) was superior in predicting mid-day NEE with an RMSE of 0.3 mgC/m^{2}s. Both models were much more precise in NEE estimation than either the NDVI*PAR technique or the NDVI*sPRI*PAR.

Conclusions

1. Chlorophyll concentrations in crops are related closely to net carbon dioxide ecosystem exchange in irrigated and rainfed maize and soybean.
2. The conceptual model, developed originally for pigment concentration retrieval in plant leaves, has been used to accurately estimate remotely chlorophyll concentrations in crops at canopy/community levels and net carbon dioxide exchange in irrigated and rainfed soybean at the field level. The technique developed and tested is solely based on remotely sensed data, and provides a robust estimate of NEE in crops.
3. Given the substantial improvement in variation explained by either of these techniques over the currently used methods (Figs. 2 and 4), it is worthwhile to explore more fully the efficacy of these techniques over different crops, at different sites, and through remote as opposed to proximal spectral sensors.
4. Further validation of this technique over other crops and vegetation types is required using the green and NIR bands of satellite-based systems such as MODIS, Landsat TM and ETM, as well as the red-edge and NIR bands of satellite systems such as MERIS and Hyperion (onboard EO-1 satellite). With further validation (e.g. in already established FluxNet and SpecNet sites), this technique may be found useful in a variety of terrestrial ecosystems. The end result may be an inexpensive yet accurate tool for estimating NEE.

Acknowledgements

This research was supported partially by the U.S. Department of Energy: (a) EPSCoR program, Grant No. DE-FG-02-00ER45827 and (b) Office of Science (BER), Grant No. DE-FG03-00ER62996. We acknowledge the support and the use of facilities and equipment provided by the Center for Advanced Land Management Information Technologies (CALMIT), University of Nebraska-Lincoln. We also wish to thank Rick Perk, Jared Burkholder and Nick Emanuel for assistance with data collection.

References

Asrar, G., M. Fuchs, E.T. Kanemasu, and J.H. Hatfield, 1984. Estimating absorbed photosynthetic radiation and leaf area index from spectral reflectance in wheat. *Agron. J.* 76:300-306.

Asrar, G., R. B. Myneni, and B. J.Choudhury. 1992. Spatial heterogeneity in vegetation canopies and remote sensing of absorbed photosynthetically active radiation: a modeling study. *Remote Sens. Environ.* 41:85–103.

Baldocchi DD, Hicks BB, Meyers TP (1988) Measuring biosphere-atmosphere exchanges of biologically related gases with micrometeorological methods. *Ecology*, 69(5), 1331-1340.

Box, E. O., 1978, Geographical dimensions of terrestrial net and gross primary productivity, *Radiation and Environmental Biophysics* 15: 305-322.

Buschmann, C. and E. Nagel. 1993. In vivo spectroscopy and internal optics of leaves as basis for remote sensing of vegetation. *Intl. J. Remote Sens.* 14: 711-722.

Cao, M. & F. I. Woodward, 1998, Dynamic responses of terrestrial ecosystem carbon cycling to global climate change, *Nature* 393: 249-252.

Dixon, R.K., S. Brown, R. A. Houghton, A. M. Solomon, M. C. Trexler & J. Wisniewski, 1994, Carbon pools and flux of global forest ecosystems, *Science* 263:185-190.

Gallo, K.P., C.S.T. Daughtry and M.E. Bauer. 1985. Spectral estimation on absorbed photosynthetically active radiation in corn canopies. *Remote Sens. Environ.* 17:221-232.

Gamon, J.A., J. Penuelas and C.B. Field, 1992. A narrow waveband spectral index that tracks diurnal changes in photosynthetic efficiency. *Remote Sens. Environ.* 4:35-44.

Gitelson, A.A. and M. Merzlyak, 1994. Spectral reflectance changes associated with autumn senescence of Asculus hippocastanum and Acer platanoides leaves. Spectral features and relation to chlorophyll estimation. *J. Plant Physiol.* 143, pp. 286-292.

Gitelson, A. and Merzlyak, M. 1996. Signature analysis of leaf reflectance spectra: algorithm development for remote sensing of chlorophyll. *J. Plant Physiol.*, 148, 495-500.

Gitelson, A., Kaufman, Y., and Merzlyak, M. 1996. Use of a Green Channel in Remote Sensing of Global Vegetation from EOS-MODIS. *Remote Sens. Environ*, Vol. 58, 289-298.

Gitelson, A.A., Merzlyak, M.N., and Chivkunova, O.B. 2001. Optical properties and non-destructive estimation of anthocyanin content in plant leaves, *Photochemistry and Photobiology*, 74(1), 38-45.

Gitelson, A.A., Zur, Y., Chivkunova, O.B. and Merzlyak, M.N. 2002. Assessing Carotenoid Content in Plant Leaves with Reflectance Spectroscopy, *Photochemistry and Photobiology*, 75(3), 272-281.

Gitelson, A.A., Gritz, U. and Merzlyak M.N. 2003. Relationships between leaf chlorophyll content and spectral reflectance and algorithms for non-destructive chlorophyll assessment in higher plant leaves. *J Plant Physiol*, Vol. 160, No 3, 271-282.

Gitelson, A. A., S. B. Verma, A. Viña, D. C. Rundquist, G. Keydan, B. Leavitt, T. J. Arkebauer, G. G. Burba and A. E. Suyker. 2003a. Novel technique for remote estimation of CO_2 flux in maize. *Geophys. Res. Lett.* 30 (9) 1486. doi:10.1029/2002GL016543.

Gitelson, A. A., A. Viña, T. J. Arkebauer, D. C. Rundquist, G. Keydan, and B. Leavitt, 2003b, Remote estimation of leaf area index and green leaf biomass in maize canopies, *Geophys. Res. Lett.* 30 (5) 1248, doi:10.1029/2002GL016450.

Goward, S.N. and K. F. Huemmrich, K.F. 1992. Vegetation canopy PAR absorptance and the normalized difference vegetation index: an assessment using the SAIL model. *Remote Sens. Environ.* 39:119-140.

Hatfield, J.L., G. Asrar, and E.T. Kanemasu. 1984. Intercepted photosynthetically active radiation estimated by spectral reflectance. *Remote Sens. Environ.* 14:65-75.

Jackson R. D., T. R. Clarke, and M. S. Moran, 1992, Bidirectional calibration results for 11 Spectralon and 16 $BaSO_4$ reference reflectance panels, *Remote Sens. Environ.* 40: 231-239.

Jarvis, P.G., and J.W. Leverenz, 1983. Productivity of temperature, deciduous and evergreen forests, in *Encyclopedia of Plant Physiology*, new series, vol. 12d, edited by O.L. Lange, P.S. Nobel, C.B. Osmond, and H. Ziegler, pp.233-280, Springler-Verlag, New York.

Kanemasu, E. T. 1974. Seasonal canopy reflectance patterns of wheat, sorghum and soybean. *Remote Sens. Environ.* 3: 43-47.

Kumar M. and J. L. Monteith. 1981. Remote sensing of crop growth. In: H. Smith (Ed) *Plants and the daylight spectrum*. Academic Press, San Diego, California. pp. 133-144.

Kumar, R. and L. Silva. 1973. Light ray tracing through a leaf cross section. *Applied Optics* 12: 2950-2954.

Lal, R., J. M. Kimble, R.F. Follett, and C. V. Cole. 1998. The potential of U.S. cropland to sequester carbon and mitigate the greenhouse effect. Ann Arbor Press, Chelsea, MI, 442 p.

Lichtenthaler, H. K. 1987. Chlorophylls and carotenoids: pigments of photosynthetic biomembranes. *Methods Enzimol.* 148: 350-382.

Lieth, H. and R.H. Whittaker. 1975. Primary Production of the Biosphere, Springer-Verlag, New York. 339 p.

Monteith, J. L., Solar radiation and productivity in tropical ecosystems, *J. Appl. Ecol.*, 9, 744-766, 1972.

Prince, S. D. and S. N. Goward. 1995. Global primary production: A remote sensing approach. *J. Biogeography* 22:815–835.

Rahman, A. F., V. D. Cordova, J. A. Gamon, H. P. Schmid, and D. A. Sims. 2004. Potential of MODIS ocean bands for estimating CO2 flux from terrestrial vegetation: A novel approach. *Geophys. Res. Lett.*, Vol. 31, L10503, doi:10.1029/2004GL019778.

Roujean, J-L. and F-M. Breon. 1995. Estimating PAR absorbed by vegetation from bidirectional reflectance measurements. *Remote Sens. Environ.* 51:375-384.

Ruimy, A., B. Saugier and G. Dedieu. 1994, Methodology for the estimation of terrestrial net primary production from remotely sensed data. *J. Geophys. Res.* 99:5263–5283.

Ruimy, A., L. Kergoat and A. Bondeau. 1999. Comparing global models of terrestrial net primary productivity (NPP): Analysis of differences in light absorption and light-use efficiency. *Global Change Biol.* 5:56–64.

Rundquist, D. C., R. Perk, B. Leavitt, G. P. Keydan and A. A. Gitelson. 2004, Collecting spectral data over cropland vegetation using machine-positioning versus hand-positioning of the sensor, *Computers and Electronics in Agriculture* 43:173-178.

Running, S. W., P.E. Thornton, R. Nemani and J.M. Glassy. 2000. Global terrestrial gross and net primary productivity from the Earth Observing System. In: O.E. Sala, R.B. Jackson, H.A. Mooney and R.W. Howarth (Eds.). *Methods in ecosystem science*. Springer, New York. pp. 44–57.

Schlesinger, W. H., 1991, Biogeochemistry: an analysis of global change, Academic Press, San Diego, CA.

Suyker, A.E., and S.B. Verma. 2001. Year-round observations of the net ecosystem exchange of carbon dioxide in a native tallgrass prairie. *Global Change Biol.* 7:279-289.

Suyker, A.E., S.B. Verma, G.G. Burba, T.J. Arkebauer, D.T. Walters, and K.G. Hubbard, 2004, Growing season carbon dioxide exchange in irrigated and rainfed maize, *Agriculture and Forest Meteorology*, 124:1-13.

Thomas, J. R. and H. W. Gaussman. 1974. Leaf reflectance vs. leaf chlorophyll and carotenoid concentration for eight crops. *Agron. J.* 69: 799-802.

USDA NASS, 1999. United States 1997 Census of Agriculture. U.S. Department of Agriculture. National Agricultural Statistics Service.

Verma, S. B., 1990, Micrometeorological methods for measuring surface fluxes of mass and energy, *Remote Sensing Reviews* 5: 99-115.

Viña, A., A.A. Gitelson, D. C. Rundquist, G.P. Keydan, B. Leavitt, J. Schepers. 2004. Monitoring Maize (Zea mays L.) Phenology with Remote Sensing. *Agronomy Journal*, Vol. 96, 1139-1147.

Walter-Shea, E.A., J. Privett, D. Cornell, M.A. Mesarch and C.J. Hays. 1997. Relations between directional spectral vegetation indices and leaf area and absorbed radiation in alfalfa. *Remote Sens. Environ.* 61:162-177.

Wofsy, S.C., M. L. Goulden, J. W. Munger, S.-M. Fan, P. S. Bakwin, B. C. Daube, S. L. Bassow, and F. A. Bazzaz. 1993, Net exchange of CO_2 in a midlatitude forest. *Science* 260:1314-1317.